

Supporting Information

**The Force of MOFs: The potential of Switchable Metal-Organic Frameworks as solvent
stimulated actuators**

Pascal Freund^{a,§}, Irena Senkowska^a, Bin Zheng^{b,c}, Volodymyr Bon^a, Beate Krause^d, Guillaume Maurin^b, and Stefan Kaskel^{, a}*

^a Inorganic Chemistry I, Technische Universität Dresden, Bergstraße 66, 01062 Dresden, Germany

^b ICGM, Univ. Montpellier, CNRS, ENSCM, Montpellier, France

^c School of Materials Science and Engineering, Xi'an University of Science and Technology, Xi'an 710054, PR China

^d Leibniz-Institut für Polymerforschung Dresden e.V., Hohe Straße 6, 01069 Dresden, Germany

* E-Mail: stefan.kaskel@tu-dresden.de

§ current affiliation: Trevira GmbH, Forster Str. 54, 03172 Guben, Germany, e-mail: Pascal.Freund@trevira.com

1. Synthesis and characterisation of MOFs

Materials. All used solvents and reagents were purchased from commercial suppliers, at least of analytical grade and used without further purification.

Synthesis of MIL-53(Al). In a slightly modified synthesis route published by Loiseau *et al.*¹, Al(NO₃)₂·9H₂O (14.13 g, 37.6 mmol) and terephthalic acid (H₂bdc) (3.13 g, 18.8 mmol) were mixed in 55 mL deionized water in a 250 mL Teflon-inlet stainless steel autoclave and heated at 493 K for one day. The subsequent washing was done according to Trung *et al.*² with minor modifications to avoid the formation of the metal oxide byproduct. Therefore, the as synthesized white product was washed with water (3 times) before suspended in 150 mL DMF and heated at 403 K overnight. The cooled product was then washed again with 150 mL DMF, filtered and calcined for 72 h at 603 K in air.

Expansion-Force Measurements. Using a customized force-measurement set up at the Leibniz Institute of Polymer research Dresden³, around 40 mg of MOF was transferred in the cylinder and pressed with different pressures to obtain various packing densities for each measurement (one point in the diagram). The pressure stamp was then lifted up 0.1 mm above the pressed powder to set the measurable pressure to 0. After adding 1 mL of solvent, the pressure resulting from the expansion of MOF was measured for at least 6 minutes until it stopped rising.

Powder X-ray diffraction. The crystallinity and phase purity of all MIL-53(Al) batches was confirmed by powder X-ray diffraction measurements. The PXRD patterns were collected on STOE Stadi P diffractometer in transmission geometry using monochromatic CuK α 1 radiation ($\lambda = 1.540562 \text{ \AA}$), MYTHEN® detector and spinning flatbed sample holder. The ω -2 θ scans were performed in 2 θ range 3-35° with 0.015° steps.

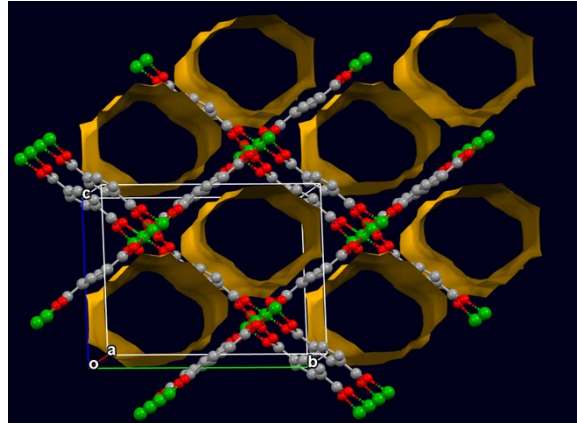
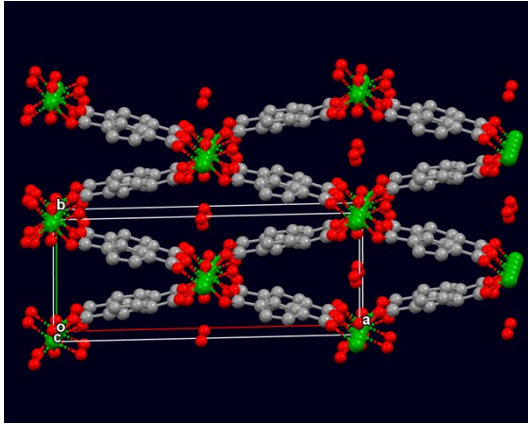


Figure S1. Crystal structure of MIL-53(Al) in the *np* form where the pores are filled with water (left) and empty *lp* form (right). Color code: Al – green, C – grey, O –red. H atoms are omitted. The solvent accessible void is indicated in yellow.

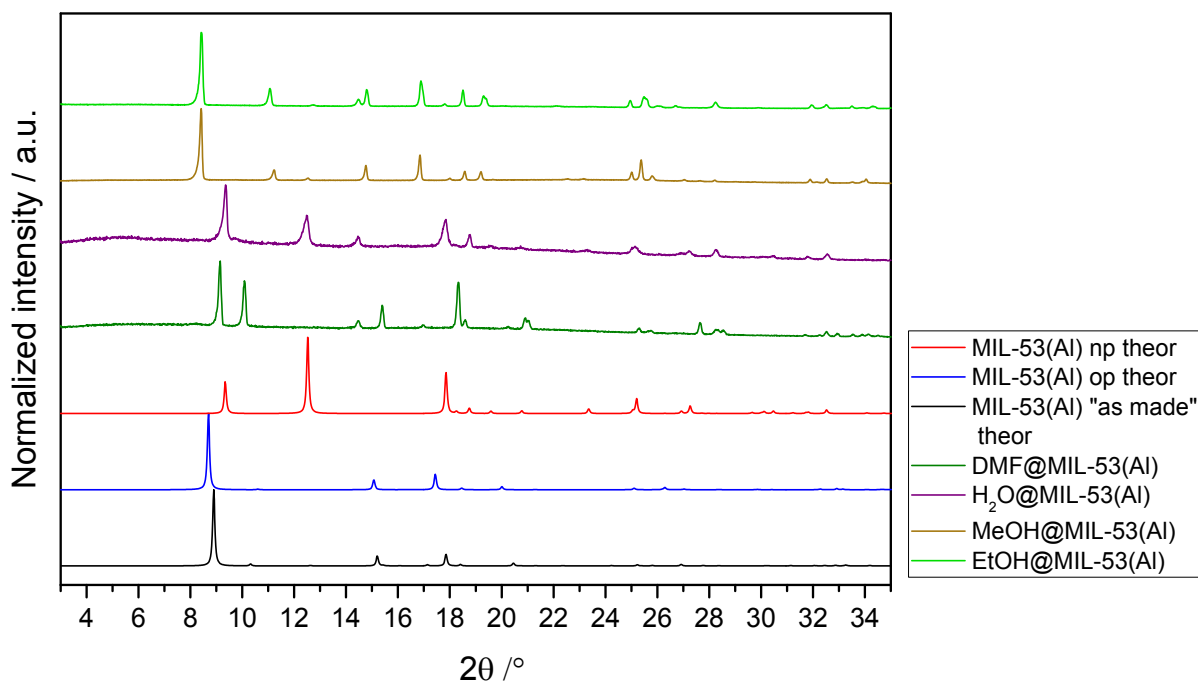


Figure S2. X-ray diffraction pattern of MIL-53(Al): theoretical pattern (CCDC 220475) of as-made compound (black); theoretical pattern (CCDC 220476) of guest free *op* form (blue), theoretical pattern (CCDC 220477) of the compound in the *np* form (red); experimental pattern of MIL-53(Al) conditioned on air for 48 h (purple); experimental pattern of compound soaked with methanol (yellow), ethanol (light green) and DMF (dark green).

Since PXRD patterns measured on DMF@MIL-53(Al), MeOH@MIL-53(Al) and EtOH@MIL-53(Al) do not match to any known MIL-53(Al) phases, the unit cells for these phases were determined *ab initio* using X-Cell program and refined using Le Bail profile fit. The refined unit cell parameters are given in Table 1.

Table S1. Unit cell parameters for the MIL-53(Al) phases.

Phase ID	Space group	$a / \text{Å}$	$b / \text{Å}$	$c / \text{Å}$	$B / ^\circ$	$V / \text{Å}^3$
MIL-53(Al) “as made” (CCDC 220475)	<i>Pnma</i>	17.129(2)	6.6284(6)	12.1816(8)	90	1383.1(2)
MIL-53(Al) <i>ht</i> (CCDC 220477)	<i>Imma</i>	6.6085(9)	16.675(3)	12.813(2)	90	1412.0(4)
MIL-53(Al) <i>lt</i> (CCDC 220476)	<i>Cc</i>	19.513(2)	7.612(1)	6.576(1)	104.24(1)	946.8(1)
DMF@MIL-53(Al)	<i>Cc</i>	18.618(1)	11.598(1)	6.6234(2)	109.585(6)	1347.5(1)
MeOH@MIL-53(Al)	<i>Imma</i>	6.6285(1)	15.7716(1)	14.1305(1)	90	1477.43(2)
EtOH@MIL-53(Al)	<i>Imma</i>	6.6239(1)	15.9738(1)	13.8902(6)	90	1469.7(1)

The crystal structure of MeOH@MIL-53(Al) was refined by Rietveld method. The initial model of MIL-53(Al) with four molecules of methanol per aluminum atom was constructed in Materials Studio software.⁴ The refinement of the crystal structure was performed using the reflex tool of the software. The methanol molecules in the pores were refined using rigid body without further restrictions.

Experimental data for MeOH@MIL-53(Al): Al(OH)(C₈H₄O₄)·4CH₃OH, Orthorhombic, *Imma*, $a = 6.62853(21) \text{ Å}$, $b = 15.77653(54)$, $c = 14.12801(48)$, $V = 1477.43(2) \text{ Å}^3$, Thompson-Cox-Hastings profile function, $U = 0.00918$, $V = 0.00392$, $W = 0.00546$, $X = -0.09872$, $Y = 0.07250$, Berar-Baldinozzi asymmetry correction $P_1 = -0.12279$, $P_2 = -0.02810$, $P_3 = -0.00001$, $P_4 = 0.00002$, $2\theta = 3 - 90^\circ$, $R_{wp} = 0.0685$, $R_p = 0.0443$.

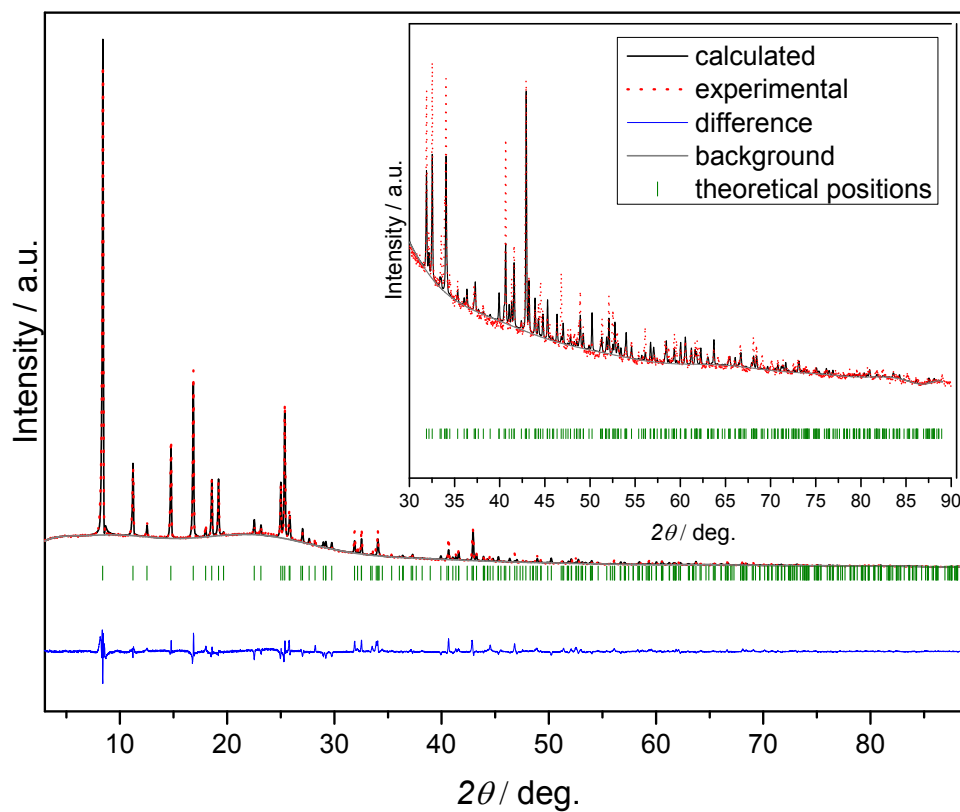


Figure S3. Rietveld plot for MIL-53(Al)·4CH₃OH.

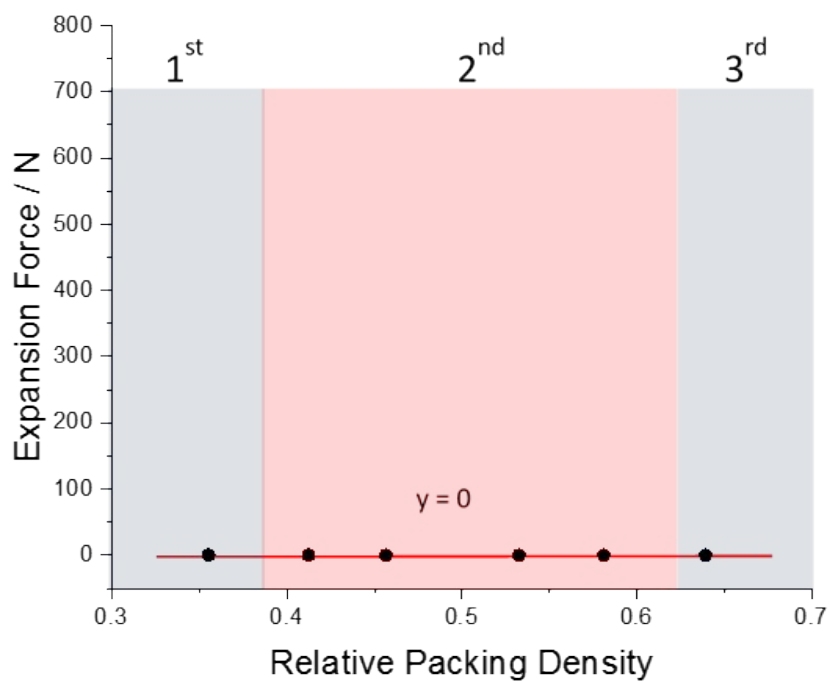


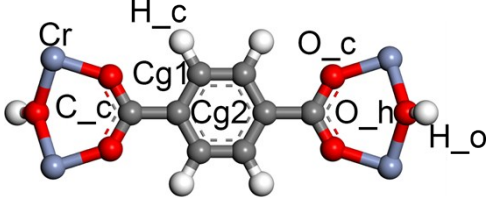
Figure S4. Expansion force measurement of MIL-53(Al) and water showing no measurable force.

2. Computational Model and Method

A simulation box made of $2 \times 4 \times 4$ MIL-53(Cr) large pore (LP) unit cells⁵ (resulting in a total of 2432 atoms in the framework) was first constructed starting with the crystal structure previously reported⁵ and further saturated with methanol considering the loading experimentally observed.⁶ The DL_POLY_2.20 program⁷ was further employed to perform Molecular Dynamics (MD) simulations at different mechanical pressure to follow the evolution of the unit cell volume as a function of the applied (and release) mechanical pressure. The Verlet-velocity integration algorithm with a time step of 1.0 fs was used. The system was thermally equilibrated at 295 K for 1 ns using $N\sigma T$ ensemble to allow the simulation box to change both size and shape, followed by 10 ns production. The thermostat and anisotropic barostat of Berendsen (with $\tau_T = 1.0$ ps and $\tau_p = 5.0$ ps as relaxation times) were employed in order to maintain constant pressure and temperature. These calculations allowed to carefully characterize the structure transition assisted by methanol.

The force field parameters (i.e., intra-molecular terms, van der Waals, and electrostatic interactions) for MIL-53(Cr) were taken from our previous work⁸ which refined them in an iterative manner to allow the reproduction of the reversible CO₂-induced *lp-np* structural transformation. These force field parameters reminded in Table S2 were further validated by capturing very well the reversible temperature and mechanical-pressure induced structural behavior of MIL-53(Cr) evidenced experimentally.⁸ The robustness of this flexible force field was again confirmed more recently with the prediction of the adsorption behaviors of CO₂/N₂ and CO₂/CH₄ mixtures for MIL-53(Cr)⁹ that match well the corresponding experimental data previously reported¹⁰. In the reference 9, we also demonstrated that this force field allows the description of the structural behavior of MIL-53(Cr) under the simultaneous application of guest adsorption and mechanical pressure that is in excellent agreement with that of its MIL-53(Al) analogue measured experimentally.¹⁰ TraPPE-UA⁶ model was employed to describe methanol and the cross Lennard-Jones (LJ) terms were calculated using the Lorentz-Berthelot mixing rule. The methanol/MIL-53 interactions were described by the sum of electrostatic and van der Waals (LJ) contributions. All non-bonded interactions were calculated using a cutoff of 12.0 Å while the electrostatic interactions were calculated using the Ewald summation.

Table S2. Force Field parameters for MIL-53(Cr) framework.⁸



MIL-53(Cr)

Bond potential: $E_{\text{bond}} = (K/2)(r-r_0)^2$

Bond type	K (kJ·mol ⁻¹)	r_0 (Å)
Cr-O_c	2928.280	1.95
Cr-O_h	2928.280	1.95
Cg1-Cg1	4015.045	1.34
Cg2-Cg2	4015.045	1.34
Cg2-C_c	2943.723	1.47
O_c-C_c	4516.925	1.25

Bending potential: $E_{\text{bend}} = (K/2)(\theta-\theta_0)^2$			Dihedral: $E_{\text{proper}} = A [1 + \cos(n\varphi - \varphi_0)]$			
Angle type	K_0 (kJ·mol ⁻¹)	θ_0 (°)	type	A (kJ·mol ⁻¹)	n	φ_0 (°)
Cg1-Cg2-Cg1	753.303	120.0	Cg1-Cg2-C_c-O_c	5.0	2	180.0
Cg1-Cg1-Cg2	753.303	120.0	Cg1-C_c-O_c-Cr	20.0	2	180.0
H_c-Cg1-Cg1	309.718	120.0				
H_c-Cg1-Cg2	309.718	120.0				
Cg1-Cg2-C_c	290.319	120.0				
Cg2-C_c-O_c	569.248	120.0				
O_c-C_c-O_c	114.165	123.0				
Cr-O_c-C_c	115.819	136.0				

VDW interaction			Partial charges q (e)	
Atom	ϵ (kJ/mol)	σ (Å)		
Cg1	0.2478	3.8068	-0.0739	
Cg2	0.2478	3.8068	-0.0739	
C_c	0.2478	3.8068	+0.6120	
O_h	0.2495	3.1200	-0.6370	
O_c	0.2495	3.1200	-0.5060	
Cr	0.0627	2.6901	+1.0322	
H_o	0.0000	0.0000	+0.2910	
H_c	0.1602	2.4483	+0.1393	

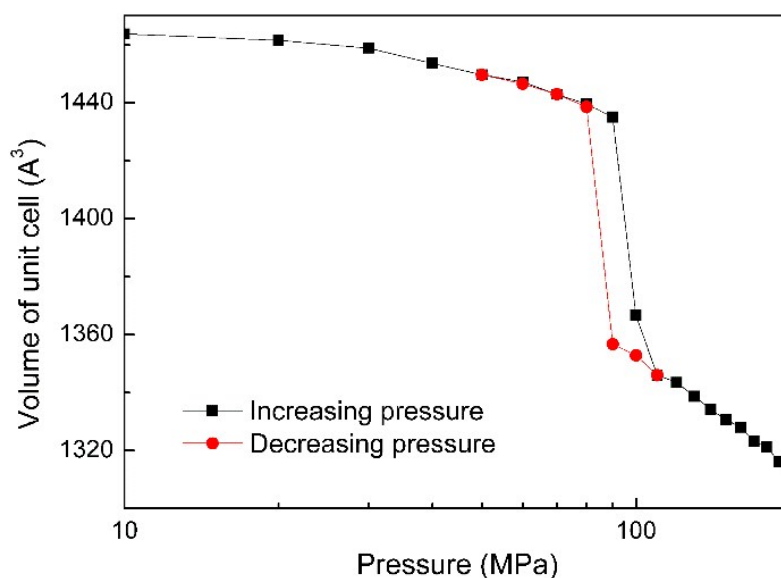


Figure S5. Evolution of the simulated unit cell volume for the methanol loaded MIL-53(Cr) as a function of the external applied pressure at 295 K.

Grand Canonical Monte Carlo (GCMC) simulations were further carried out at 298 K to compute the saturation capacities as well as the adsorption enthalpies at low coverage using the revised Widom's test particle insertion method¹¹ for both methanol and ethanol in MIL-53(Cr) open pore (*op*) by employing the Complex Adsorption and Diffusion Simulation Suite (CADSS) code.¹² We used the same simulation box as the one described above and 1×10^8 Monte Carlo steps were used for both equilibration and production runs. The host/guest interactions were described in the same manner as in the MD simulations, the ethanol molecule being represented by the same TraPPE-UA⁶ model than methanol. The saturation capacities were predicted to be 12 and 7 molecules per unit cell for methanol and ethanol respectively, which are in very good agreement with the experimental uptake reported previously.¹³

3. References

1. T. Loiseau, C. Serre, C. Huguenard, G. Fink, F. Taulelle, M. Henry, T. Bataille and G. Férey, *Chem.Eur. J.*, 2004, **10**, 1373-1382.
2. T. K. Trung, P. Trens, N. Tanchoux, S. Bourrelly, P. L. Llewellyn, S. Loera-Serna, C. Serre, T. Loiseau, F. Fajula and G. Férey, *J. Am. Chem. Soc.*, 2008, **130**, 16926-16932.
3. B. Krause, R. Boldt, L. Häußler and P. Pötschke, *Compos. Sci. Technol.*, 2015, **114**, 119-125.
4. Materials Studio 5.0; Accelrys Software Inc.: San Diego, CA, USA, 2009.
5. C. Serre, F. Millange, C. Thouvenot, M. Noguès, G. Marsolier, D. Louër and G. Férey, *J. Am. Chem. Soc.*, 2002, **124**, 13519-13526.
6. B. Chen, J. J. Potoff and J. I. Siepmann, *J. Phys. Chem. B*, 2001, **105**, 3093-3104.
7. W. Smith and T. R. Forester, *J. Mol. Graph.*, 1996, **14**, 136-141.
8. A. Ghoufi, A. Subercaze, Q. Ma, P. G. Yot, Y. Ke, I. P. Orench, T. Devic, V. Guillerme, C. Zhong, C. Serre, G. Férey and G. Maurin, *J. Phys. Chem. C* 2012, **116**, 13289-13295.
9. N. Chanut, A. Ghoufi, M.V. Coulet, S. Bourrelly, B. Kuchta, G. Maurin, P.L. Llewellyn, *Nat. Commun.* 2020, **11**, 1216.
10. L. Hamon, P. L. Llewellyn, T. Devic, A. Ghoufi, G. Clet, V. Guillerme, G. D. Pirngruber, G. Maurin, C. Serre, G. Driver, W. van Beek, E. Jolimaître, A. Vimont, M. Daturi and G. Férey, *J. Am. Chem. Soc.* **2009**, *131*, 17490-17499.
11. T. J. H. Vlugt, E. García-Pérez, D. Dubbeldam, S. Ban and S. Calero, Computing the Heat of Adsorption using Molecular Simulations, *J. Chem. Theory Comput.*, 2008, **4**, 1107-1118
12. Q. Yang, C. Zhong, *J. Phys. Chem. B* 2006, **110**, 36, 17776-17783
13. S. Bourrelly, B. Moulin, A. Rivera, G. Maurin, S. Devautour-Vinot, C. Serre, T. Devic, P. Horcajada, A. Vimont, G. Clet, M. Daturi, J.-C. Lavalley, S. Loera-Serna, R. Denoyel, P. L. Llewellyn and G. Férey, *J. Am. Chem. Soc.*, 2010, **132**, 9488-9498.